Composites: Part A 173 (2023) 107673

Contents lists available at ScienceDirect

Composites Part A

journal homepage: www.elsevier.com/locate/compositesa

3D MXene frameworks for flame retardant hydrophobic polymer nanocomposites

Wei Wang [b,*], Cheng Wang [b], Anthony Chun Yin Yuen [d], Ao Li [b], Bo Lin [b], Yao Yuan [c], Chao Ma [a,*], Yu Han [e,*], Guan Heng Yeoh [b]

[a] College of Emergency Management, Nanjing Tech University, Nanjing 211816, China
[b] School of Mechanical and Manufacturing Engineering, University of New South Wales, Sydney, NSW 2052, Australia
[c] Fujian Provincial Key Laboratory of Functional Materials and Applications, School of Materials Science and Engineering, Xiamen University of Technology, Xiamen 361024, China
[d] Department of Building Environment and Energy Engineering, The Hong Kong Polytechnic University, Hong Kong Special Administrative Region
[e] School of Mechanical Engineering and Automation, Northeastern University, Shenyang 110819, China

ARTICLE INFO

Keywords:
MXene
Flame retardancy
PVB composites
Synergistic effect
Fire safety

ABSTRACT

MXene has been the subject of various studies and applications in polymer composites in recent years. However, its compatibility with hydrophobic polymers has been a significant limitation. This study presents a simple way to create MXene frameworks to realise flame retardant hydrophobic polymer composites. The fabrication process is environmentally friendly and low-cost. The PVB/HPUPO/MXene composite membrane showed a 74.7% reduction in volatile intensity during thermal degradation compared to pristine PVB. The PVB/HPUPO/MXene composite membrane also demonstrated significantly improved flame retardancy compared to pure PVB. Specifically, MXene based networks and HPUPO showed synergistic effect in improving the fire safety of PVB composites. This study offers a new approach to incorporating MXene as a flame retardant into conventional phosphorus- and nitrogen-based flame retardant systems for hydrophobic polymers with great fire retardancy.

1. Introduction

In the last few years, $Ti_3C_2T_x$ MXene nanosheets have attracted intensive attention due to their unique properties and have already been successfully applied in polymer composites for improved performance, such as thermal stability, flame retardancy, electromagnetic interference (EMI) shielding properties[1–3]. In terms of the additives for polymer matrix, MXene as two-dimensional transition metal carbides and/or nitrides nanosheets shows a high specific surface area and outstanding electrical conductivity that may construct conductive networks to achieve desired properties such as EMI shielding and thermo-electrical performance[4–7]. In addition, the well dispersion of MXene in polymer substrates may also facilitate the performance of thermals stability, mechanical performance, and flame retardancy. Indeed, MXene has already demonstrated the ability to enhance polymer matrix with significantly improved properties. However, as we know, MXene nanosheets, due to the hydrophilicity feature, can only be well dispersed in water and a limited number of other solvents and thus be highly restricted in the application of polymers that can only be dissolved in organic solvents.

Many efforts have been dedicated to enhancing the polymer composites such as poly vinyl alcohol (PVA)[8,9], polystyrene (PS)[10], polyurethane (PU)[11,12], polypropylene (PP)[13], etc., by utilising MXene nanosheets. Usually, MXene nanosheets are more likely to be employed to improve the performance of water-soluble polymers like PVA, as they can all achieve well dispersions in water and form a homogeneous solution. Therefore, the conventional mixing method of MXene nanosheets and polymer matrix could be inappropriate for the application in non-water-soluble polymers like PS, PP, and PE. Yu et al prepared MXene@PS nanocomposites by using electrostatic assembly method to achieve enhanced performance[14]. In this work, MXene nanosheets are fabricated on the surface of PS nanospheres, and the high-performance MXene@PS nanocomposites are obtained by the mould pressing method. Yu also prepared MXene/natural rubber nanocomposites by the same principle[15]. Here the natural rubber is water-soluble and can maintain a stable suspension in water. Because of the electrostatic repulsion, the negative charges of MXene nanosheets and natural rubber particles promote the formation of homogeneous

* Corresponding authors.
E-mail addresses: wei.wang15@unsw.edu.au (W. Wang), machaoyjgl@njtech.edu.cn (C. Ma), yuhan.neu@gmail.com (Y. Han).

https://doi.org/10.1016/j.compositesa.2023.107673
Received 18 April 2023; Received in revised form 13 June 2023; Accepted 28 June 2023
Available online 29 June 2023

MXene/natural rubber dispersion. And the MXene/natural rubber membrane can be obtained after the filtration process. In addition, MXene nanosheets may also be coated on the surface of PP textiles with improved performance[16]. In this work, PP textile is pre-treated by the oxygen plasma technique to obtain a charged surface, and then modified by polyethyleneimine solution to form a positive charged surface that could interact with negative charged MXene coating. Similarly, Zhao et al also utilised the modified MXene as the coating to enhance the performance of PP nonwoven fabrics for improved thermal stability and flame retardancy[13]. Many efforts using the similar methods have been studied to realise high-performance MXene/polymer nanocomposites and membranes. Nevertheless, the self-assembly method of MXene and polymer particles followed by the hot compression and the filtration method make the fabrication process complicated and high cost.

The critical point of the methods employed to prepare MXene/polymer nanocomposites is to resolve the poor dispersion of MXene in polymers especially for hydrophobic polymers. As we all know, MXene nanosheets can be well dispersed in water and precipitate in most organic solvents. Due to this, the MXene networks prepared by the above methods can hardly be used to fabricate flame retardant nanocomposites with a low cost and feasible procedure when using organic solvents. Hence, it is nearly impossible to disperse the MXene nanosheets well in hydrophobic polymers without modifications. Unfortunately, up to now, there are limited reports introducing practical approaches to constructing high-performance 3D networks for hydrophobic polymers.

In this work, we introduce a simple freeze-drying method to synthesise 3D MXene frameworks that could significantly improve the flame retardancy of hydrophobic polymer nanocomposites. In order to explore the applicability of MXene frameworks in existing flame retardant systems, we will combine them with phosphorus and nitrogen-based flame retardants to enhance the fire safety of polymer composites. Currently, most commercial flame retardants are organic compounds that incorporate phosphorus, nitrogen, and halogens, such as ammonium polyphosphate, etc. In this study, we will incorporate hyperbranched poly(urethane-phosphine oxide) (HPUPO) along with MXene frameworks to synergistically improve flame retardancy. Different from the previously reported methods, this work has no chemical modification for MXene nanosheets and no chemical or electrostatic interactions among the components. Moreover, poly vinyl alcohol (PVA) as a healthy and degradable hydrophilic polymer was used here to help architect the structure of 3D MXene frameworks. The incorporation of PVA will help improve the stability of the 3D frameworks and, to some extent, the compatibility with other polymers. The flame retardant MXene/polymer nanocomposites were prepared by combining the 3D MXene frameworks and hydrophobic polymer polyvinyl butyral (PVB) by a simple dipping process. In summary, the flame retardant PVB/HPUPO/MXene nanocomposites introduced in this work have four main advantages over existing methods: 1) there are no chemical modification and complicated reaction conditions required during the composites fabrication procedure which is very green and environmentally friendly. Also, employing PVA as the binder will make the 3D MXene networks more stable, sustainable, and recyclable, as the MXene/PVA system can be completely well dispersed/dissolved in hot water and reused when reaching the use period. 2) The feasible fabrication process with no chemical reaction and using toxic organic solvents will allow this kind of 3D MXene/PVA networks with low cost and practical potential. 3) These unique 3D MXene networks coated by PVA resin are compatible with PVB-ethanol solution and exhibit wide application potential in various hydrophobic polymers with improved flame retardancy. As we know, MXene nanosheets are usually prone to be oxidised to titanium dioxides. In this work, MXene networks will be protected by a thin PVA resin and can be stored for long term. This feature will allow these 3D MXene networks to have wider application possibilities. 4) In this work, we also introduced conventional flame retardant (HPUPO) into the PVB matrix to study the synergistic effect of 3D MXene networks and organic flame retardant on PVB composites. The investigation would help deeply learn through the feasibility and practicality of this flame-retardant network when being employed in an organic flame retardant system, which would advance the development of current MXene-based flame retardants.

2. Experiments

2.1. Raw materials

Poly(vinyl alcohol) (PVA) (1799, 98–99%, mol/mol) and polyvinyl butyral (PVB) (M.W.170,000–250,000) were purchased from Shanghai Aladdin Biochemical Technology Co., Ltd. Hydrochloric acid (HCl, 36.0——38.0 wt% in H_2O) and lithium fluoride (LiF, AR, 99%) were bought from Sinopharm Chemical Reagent Co., Ltd. Raw Ti_3AlC_2 was provided by 11 Technology Co., Ltd. All the chemicals are used without further treatment. N, N-dimethylformamide (DMF), Dibutyltin dilaurate (DBTDL), barium oxide and methanol were bought from Sinopharm Chemical Reagent Co. Ltd., China. 4,4′-diphenylmethane diisocyanate (MDI) was supplied by Aladdin Chemistry Co. Ltd., China. Trihydroxymethylphosphine oxide (THPO) was synthesized using the reported method[17].

2.2. Synthesis of hyperbranched poly (Urethane-Phosphine Oxide) (HPUPO) and exfoliated MXene nanosheets

HPUPO was synthesized by our previous procedures[18]. Before use, DMF was dehydrated by distillation over barium oxide under a vacuum. 0.48 g DBTDL (0.76 mmol) and 24.1 g THPO (0.172 mol) were added into 250 mL anhydrous DMF under nitrogen. After dissolution, 38.0 g MDI (0.152 mol) was added to the mixture in batches. When the mixture turned into transparent solution, the reaction was kept for 48 h at room temperature. After it was poured into massive methanol (2.5 L), the solid was precipitated. The obtained solid was filtered and washed by methanol. Then it was dried in a 100 °C vacuum oven for 24 h to yield HPUPO. The detailed chemical structure and synthesis route are described in Figure S1.

The fabrication of MXene Nanosheets is prepared according to the Gogotsi method[19]. The diluted HCl solution was obtained by mixing 60 mL of concentrated HCl (12 M) and 20 mL of H_2O. Then, 4 g of LiF was added into the diluted HCl solution and well dissolved. After that, 4 g of Ti_3AlC_2 powders were added into the HCl/LiF solution under constant magnetic stirring. The etching process lasted for 48 h under 40 ℃. Here we employed a milder physical shaking method. Then, the mixtures were washed with deionized water and centrifugation without sonication until the pH value reached near 7. The precipitation should be washed and centrifugated without ultrasonication until the suspension cannot be centrifugated down below 10000 rpm. This step would last about 10 h. The last step was to use ultrasound for 30 min to redisperse the sediments in water and collect the suspension that could not be centrifugated at 7000 rpm for 5 min, removing little left unexfoliated MXene layers. The yield rate of MXene using this method can reach nearly 100%. The obtained MXene suspension has a 2.1 wt% solid concentration.

2.3. Fabrication of 3D MXene/PVA frameworks

The 3D MXene/PVA frameworks were prepared using a simple phase-change and freeze-drying method. Firstly, 2 g of PVA particles were added into 100 g of water and completely dissolved at 100 Celsius degrees. After the PVA solution cooled down, the same amount of MXene suspension was added by drop into the above solution under constant magnetic stirring. After 1 h, there would get a homogeneous MXene/PVA solution. By casting the above solution onto a steel plate and then moving the stained steel plate into an ethanol bath stably and slowly, after 2 h, a cellular and uniform MXene/PVA membrane would be precipitated in an ethanol bath. At last, the porous membrane was

move from the ethanol bath and placed into a freeze drier under −40 Celsius degrees for 30 min to remove the ethanol and water residues. Then, the dark blue porous membrane was obtained and marked as MXene/PVA.

2.4. Preparation of PVB/HPUPO/MXene

The fabrication process of PVB/HPUPO/MXene is simple and fast. First, 0.5 g of HPUPO was completely dissolved in 40 mL DMF solvent with constant magnetic stirring. Then, 9.5 g of PVB was added to the above solution. After 30 min, a transparent and clear solution could be obtained. Lastly, the prepared MXene/PVA frameworks were dipped into the above PVB/HPUPO solution. After 1 min of dipping, MXene/PVB framework filled with PVB/HPUPO solution was dried for 6 h under 60 ℃ condition. Finally, PVB/HPUPO/MXene would be obtained and ready for further characterization.

3. Results and discussion

As we know, $Ti_3C_2T_x$ MXene shows exceptional properties that are mainly attributed to its unique structures. In this work, $Ti_3C_2T_x$ MXene was prepared by a typical acid etching method shown in Fig. 1a. Moreover, reported works showed that the yield rate of $Ti_3C_2T_x$ MXene was lower than 20% if using traditional intercalation and delamination two-step synthesis.[20] In this work, a milder physical shaking method was used to wash out the Al^{3+}, acid and exfoliate the $Ti_3C_2T_x$ layer after the etching process. Notably, the sonication would not be used during the washing process. The mild shaking would not seriously damage the MXene layer, so that high-quality nanosheets can be obtained. As we know, the moving out of Al^{3+} and the exfoliation are processed slowly; hence mild treatment would maintain the shape quality and improve the yield rate. Actually, it was surprising that this method could improve the yield rate to almost 100%. It should be noted that here the yield rate was calculated very roughly, the criteria are that there is no precipitation under 7000 rpm for 5 min. The key point to achieve this high yield rate is that the washing process should be operated under mild shaking conditions for a long time simultaneously with constant washing with DI water and high-speed centrifugation.

As shown in Fig. 1b, in terms of the raw Ti_3C_2Al, the TEM image shows that there exist obvious stacked and thick layered structures. For $Ti_3C_2T_x$ MXene nanosheets, as shown in Fig. 1c, the stacked layers are thoroughly exfoliated into several large and thin nanosheets with a diameter size range from 0.4 μm − 1.0 μm. Moreover, the TEM images also demonstrate that the $Ti_3C_2T_x$ MXene nanosheets maintain high-quality shapes and have no damages whereases these damages reported in previous works are usually caused by sonication treatment. The realisation of high-quality nanosheets is probably attributed to the mild shaking method. In addition, XRD data presented in Fig. 1d also confirmed that the (001) plane of exfoliated $Ti_3C_2T_x$ MXene at 6.8° appears with enlarged interlayer spacing. Furthermore, the peaks of $Ti_3C_2T_x$ MXene at (101), (103), (104), (105), and (107) almost disappeared after the exfoliation process, which verified that Ti_3C_2Al layers

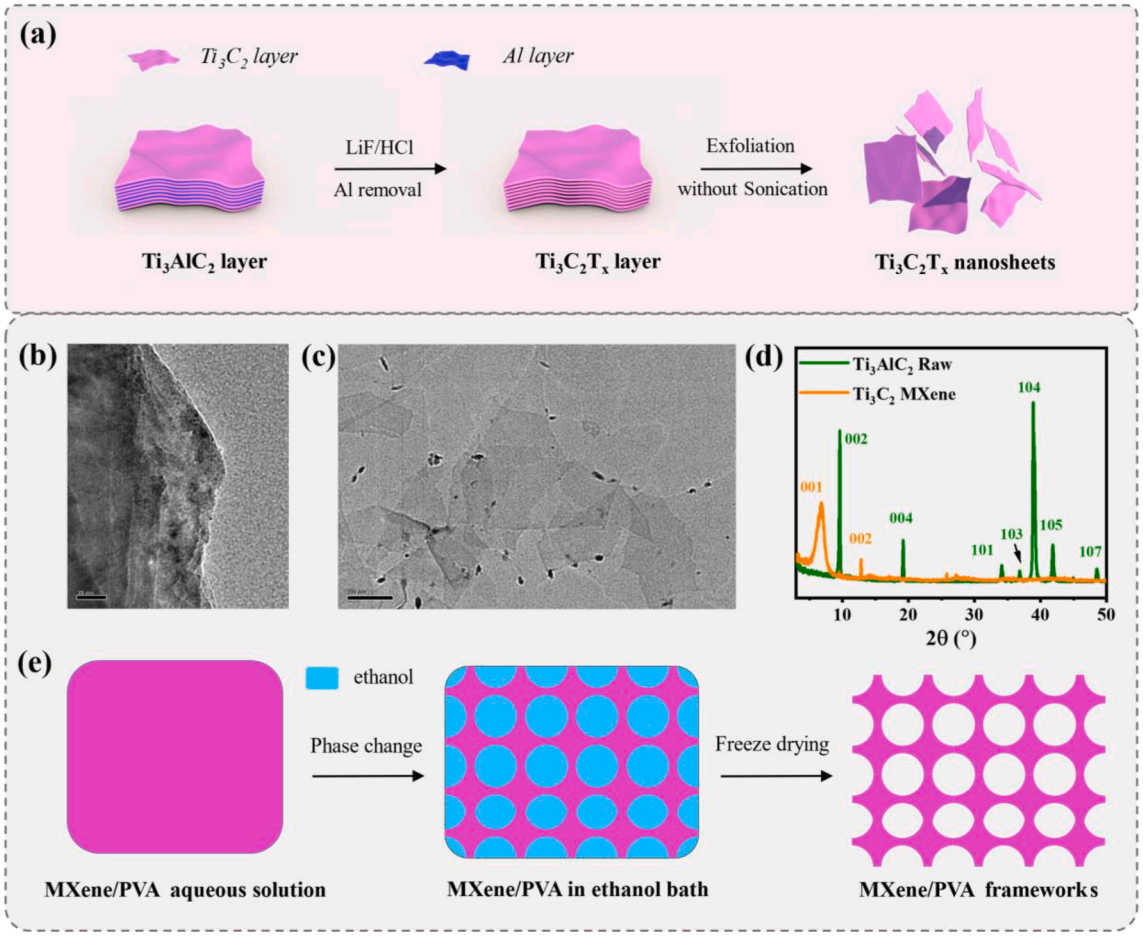

Fig. 1. The construction of the MXene/PVA framework. a) The schematic illustration of the fabrication process of MXene nanosheets through a typical acid etching method; TEM images of b) raw Ti_3AlC_2 layer and c) $Ti_3C_2T_x$ MXene nanosheets; d) XRD data of raw Ti_3AlC_2 layer and $Ti_3C_2T_x$ MXene nanosheets; e) The schematic illustration of the preparation of MXene/PVA framework using the phase change and freeze-drying methods. (For interpretation of the references to colour in this figure legend, the reader is referred to the web version of this article.)

were converted to mono-/few layered $Ti_3C_2T_x$ MXene by removing the Al layer using LiF/HCl solution and the mild shaking treatments.

MXene nanosheets can realise a great dispersion in water but cannot be compatible with hydrophobic polymers. To introduce the MXene into the hydrophobic polymer substrate for improved fire safety performance, in this work, the concept of MXene based skeleton is proposed for the first time to improve the thermal stability and flame retardancy of Polyvinyl butyral (PVB). The fabrication of MXene/MXene skeleton was prepared according to a simple two-step method. As shown in Fig. 1e, MXene and PVA may realise a homogeneous and stable solution that will change to MXene/PVA framework with high porosity near 91% when immersed into an alcohol bath by a phase change method. Then the freeze-drying method was employed to extract the excessive alcohol under a low temperature of under – 40 ℃ and retain the MXene/PVA framework. The prepared MXene/PVA framework is compatible with PVB substrate and can directly absorb PVB/HPUPO DMF based-solution. Incorporating PVB with MXene based framework can result in a thin, thermal stable, and flame retardancy PVB/HPUPO/MXene membrane.

In terms of PVB membrane with HPUPO, HPUPO may realise a great dispersion in PVB. As shown in Fig. 2a and b, due to the excellent resolution state of PVB and HPUPO in DMF solvent, the SEM images of the cross-section show smooth with no apparent aggregation. Moreover, in Fig. 2c and d, the elemental mapping images also demonstrate that phosphorus and nitrogen originated from flame retardant additive HPUPO show an even distribution signal, indicating good dispersion of HPUPO in PVB.

For the MXene/PVA framework, as shown in Fig. 2e and f, the SEM images of the cross-sectional surface show that MXene/PVA has an evenly porous structure with high porosity. Moreover, when under high resolution as presented in Fig. 2g, it may be found that the porous structure is comprised of nanosheets coated with thin polymer which are MXene and PVA respectively. In addition, the element mapping image of Ti shown in Fig. 2h also confirm the uniform distribution of MXene nanosheets. In this work, we are fabricate MXene based framework with PVA as the binder. Hence, as for this target, the SEM results can confirm the successful preparation of the MXene/PVA framework.

At last, in the case of the PVB/HPUPO/MXene membrane, as shown in Fig. 2i and j, the thickness of this membrane reduced to about 30 μm compared to MXene/PVA framework 150 μm. This thickness is similar to that of the PVB/HPUPO membrane, which is probably attributed to the flexibility of the MXene/PVA framework that allows the deformation during the PVB membrane-forming process. Moreover, the cross-section surface presents rough and uneven, which is caused by the different shear forces of the polymer substrates at the time of fracture. When zoomed in, shown in Fig. 2k, as pointed out by the white arrows, many obvious protrusions could be easily found and are generated by the facture of the MXene/PVA framework. In terms of the continuous substrate, it is PVB/HPUPO substrate. The phosphorus element mapping in Fig. 2l also confirms that phosphorus is well dispersed in the matrix that means that PVB/HPUPO component can be successfully incorporated into MXene/PVA frameworks and simultaneously realise a good compatibility.

Here we also provide the digital photos of the MXene/PVA frameworks and PVB/HPUPO/MXene membrane. As shown in Fig. 3a, the prepared MXene/PVA framework shows excellent rollability and flexibility. Moreover, in Fig. 3b, this kind of porous membrane still exhibits an ultrathin feature that may also potentially realise ultrathin polymer composites membranes. The schematic illustration of the MXene/PVA frameworks is presented in Fig. 3c. This kind of MXene-based flame retardant skeleton is proposed for the first time to be employed in hydrophobic polymer composite systems like the membrane in this work shown in Fig. 3d and 3e. PVB/HPUPO/MXene membrane also shows flexibility and ultrathin advantage.

As illustrated in Fig. 3f, after the combination of PVB/HPUPO and MXene/PVA system, the newly generated PVB/HPUPO/MXene will be protected by double insurance including flame retardant HPUPO and MXene-based frameworks. A verification experiment was carried out to demonstrate further the continuous state of PVB/HPUPO inside PVB/HPUPO/MXene. As depicted in Fig. 3g, PVB/HPUPO/MXene membrane was tailored and maintained in boiling water for 6 h, then a piece of the

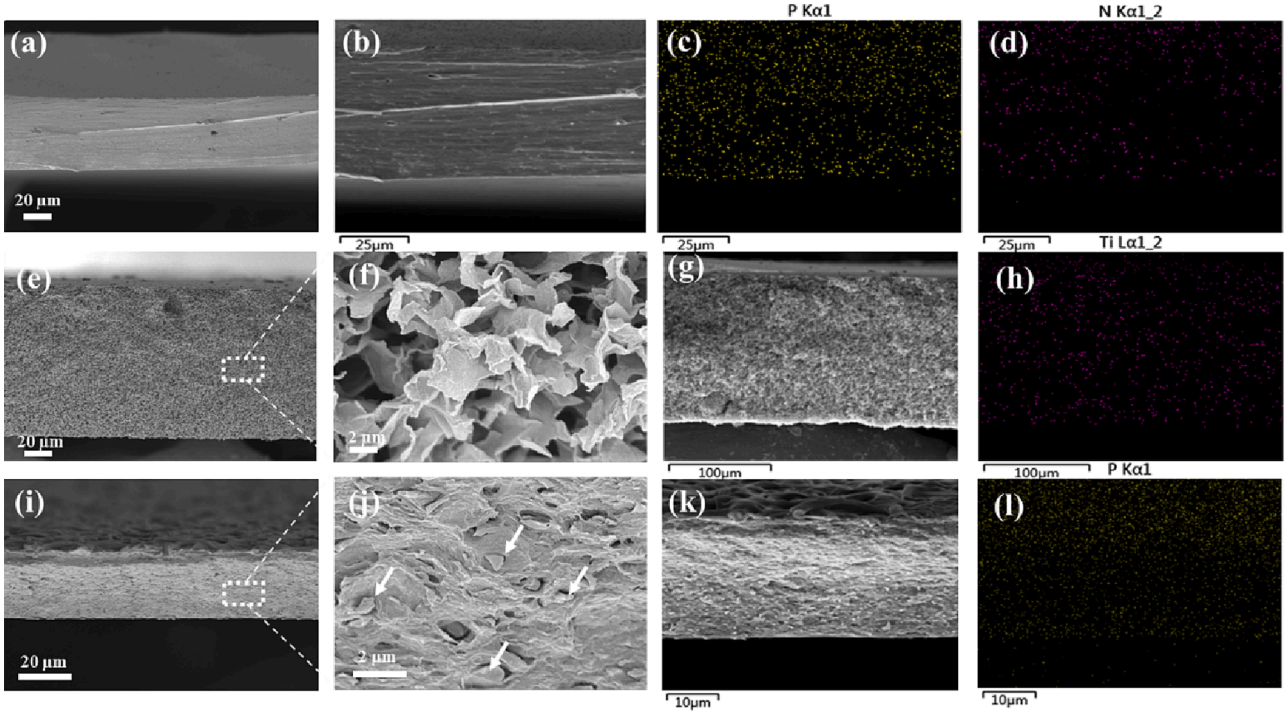

Fig. 2. The microscale structure of membranes. SEM images and element mapping images of PVB/HPUPO: a, b) cross-sectional structures, c) Phosphorus and d) nitrogen elements mapping images; MXene/PVA frameworks: e-g) SEM image of the cross-sectional surface, h) Ti element mapping image; PVB/HPUPO/MXene membrane: i-k) SEM image of cross-sectional surface, l) phosphorus element mapping images.

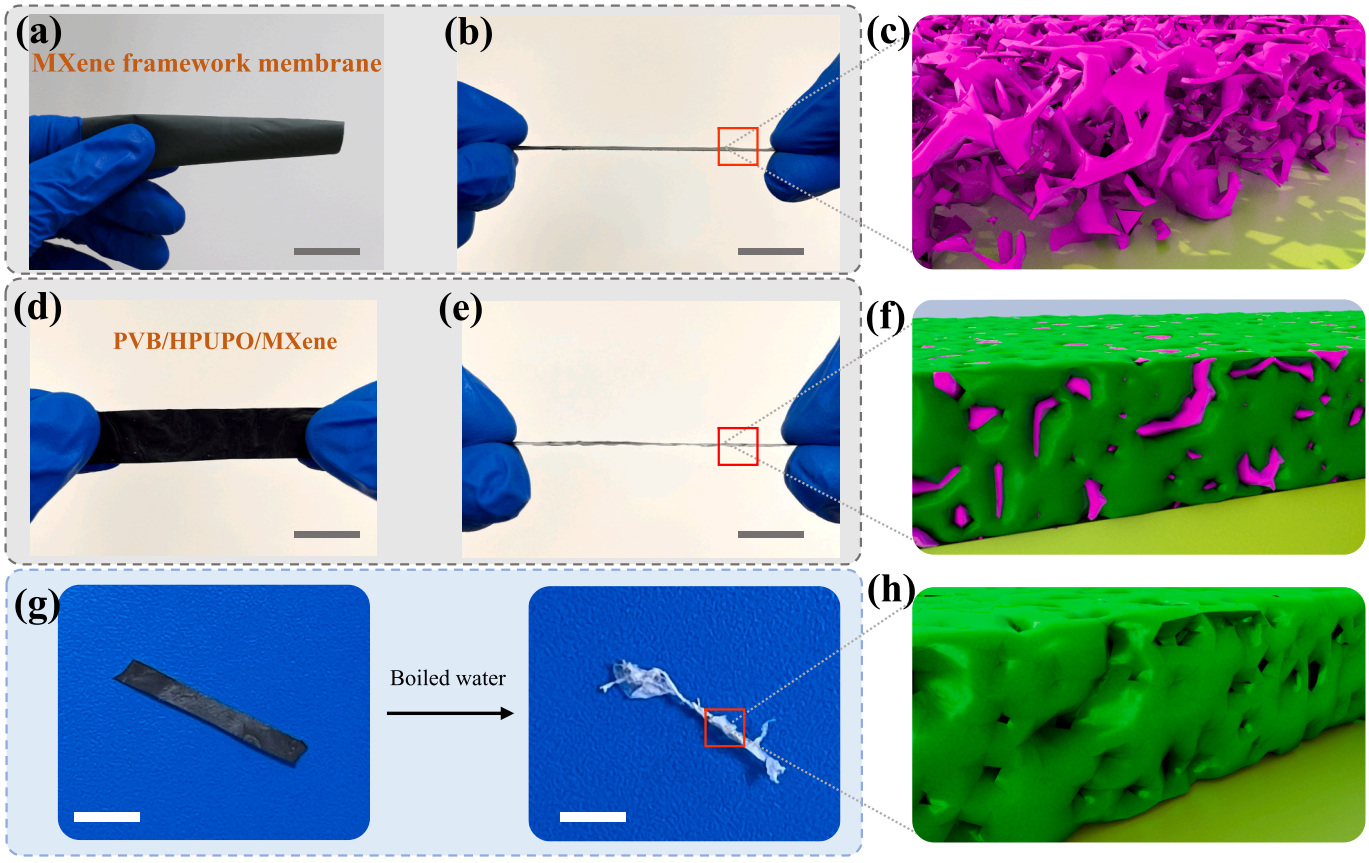

Fig. 3. A, b) digital photos and c) schematic illustration of mxene/pva membrane with a grey scale bar of 20 mm. d, e) Digital photos and f) schematic illustration of PVB/HPUPO/MXene membrane with a grey scale bar of 20 mm. g) Photos of PVB/HPUPO/MXene membrane and product after boiling for 6 h. The insert white scale bar is 15 mm. h) Schematic structure of PVB/HPUPO membrane. (For interpretation of the references to colour in this figure legend, the reader is referred to the web version of this article.)

white membrane would be obtained, which means that as illustrated in Figure h, the PVB/HPUPO matrix is continuous in the composites system.

To meet the essential requirement of mechanical performance in specific applications, polymer composite membranes are usually required to possess good tensile strength. A simple demonstration experiment shown in Fig. 4a proved that the prepared PVB/HPUPO/MXene has good mechanical properties. In fact, the MXene frameworks enhanced PVB membrane cannot achieve improved mechanical properties by using a physical mixing strategy such as the method introduced in this work. Further increasing the mechanical performance of this kind of frameworks-based composites is another challenging subject, which will be studied in the next subject. In this work, MXene-based frameworks are mainly used to enhance the thermal stability and flame retardancy of hydrophobic polymers. As presented in Fig. 4b, it can be seen that after the addition of MXene, PVA/MXene aerogel shows significantly improved thermal stability compared to pristine PVA with higher residues when under 800 ℃ about (23.0 wt%) and increased temperature of maximum degradation rate (T_{max}) near 357 ℃. Regarding pristine PVB, the main degradation process happened at the

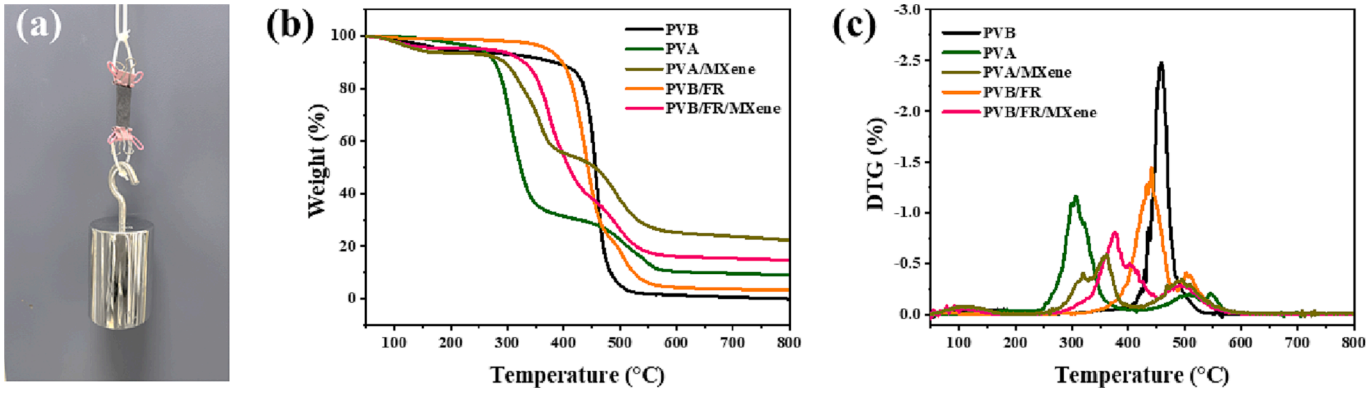

Fig. 4. Mechanical performance and thermal stability of PVB/HPUPO/MXene membrane. a) Demonstration of mechanical strength of PVB/HPUPO/MXene membrane by bearing a weight of 1000 g. The scale of the membrane: width: 10 mm; thickness: 30 μm. b) TGA and c) DTG results of PVB, PVA, PVA/MXene, PVB/HPUPO, and PVB/HPUPO/MXene membranes. (For interpretation of the references to colour in this figure legend, the reader is referred to the web version of this article.)

temperature of 458 ℃, and no residue was left at 800 ℃. Therefore, this aerogel can act as a flame retardant to further improve the fire safety of PVB composites enhanced by HPUPO. After the incorporation of HPUPO, the degradation rate of PVB/HPUPO was significantly reduced which can be confirmed by DTG data shown in Fig. 4c. Moreover, the char residue of PVB/HPUPO at 800 ℃ was also increased to 3.3 wt%. In terms of PVB/HPUPO/MXene, the residue was further obviously increased to 14.6 wt%, which was enhanced by the MXene-based frameworks. Actually, as shown in Fig. 4c, the addition of PVA in MXene/PVA frameworks may result in degradation shifting to a lower temperature. But the incorporation of MXene and flame retardant HPUPO can improve the thermal stability and alleviate the predegradation phenomenon. Nevertheless, the degradation rate of PVB/HPUPO/MXene was also the lowest among all indicating that the system comprising of MXene-based frameworks and HPUPO can effectively reduce the degradation rate and improve the thermal stability of PVB/HPUPO/MXene composite membrane.

As we all know, the fire hazards during fire accidents are mainly originated from the release of smoke and toxic volatile gases during materials combustion that may lead to fatal injury. Hence in this work we also provide the results of pyrolyzed products of the membranes during thermal degradation. As shown in Fig. 5a, in terms of the absorbance of the volatiles, PVB/HPUPO/MXene shows the lowest intensity compared to PVB (near 74.7% off), PVA, and PVB/HPUPO, which indicates that PVB/HPUPO/MXene release much lower gaseous volatiles during the thermal degradation. In addition, PVA/MXene aerogel displays the low intensity of the volatiles as well, as MXene possesses excellent flame retardancy that can decrease the thermal degradation of the PVA matrix and thus reduce the release of degraded gaseous products. Specifically, as shown in Figure b, the signal around 1100 cm^{-1} is attributed to the C-O stretching originating from PVA and PVB. The intensity of ethers for PVB/HPUPO/MXene also gets significantly reduced compared to PVB and PVB/HPUPO membranes. In addition, during the combustion, the unsaturated structure of PVB may lead to the generation of C = O structures that can result in a C = O stretching signal at a position near 1700 cm^{-1}. Surprisingly, the addition of HPUPO cannot reduce the generation of carbonyl compounds. In contrast, PVB/HPUPO/MXene shows the extremely low intensity of carbonyl compounds, probably ascribed to the MXene based frameworks that plays a critical role in the physical barrier effect. For the release of CO_2, as shown in Fig. 5d, at the position of about 2325 cm^{-1}, the generation of CO2 is also suppressed by the combination system of MXene-based frameworks and HPUPO. Similarly, HPUPO here even increases the generation of CO_2. At last, for the hydrocarbons that usually produce smoke particles located at 2730 cm^{-1} and 2950 cm^{-1}, as can be seen in Fig. 5e and 5f, HPUPO still plays antagonistic effect on the release of hydrocarbons. In comparison, PVB/HPUPO/MXene exhibits significantly reduced intensity of hydrocarbons showing promising smoke suppression potential. In the case of PVA/MXene aerogel, it shows the low tensity of released products as well as PVB/HPUPO/MXene composites. Therefore, it can be regarded that PVA/MXene networks play critical role in suppressing the release of gaseous volatiles.

In this section, it can be concluded that incorporating HPUPO can hardly significantly reduce the release of pyrolyzed volatiles. As for the MXene-based frameworks, they can tremendously reduce the intensity of all various pyrolyzed products. The above results demonstrate that MXene-based frameworks plays a critical role in suppressing the release of toxic volatiles by the gaseous phase mechanism. As designed at the beginning, MXene-based frameworks are managed to build a physical barrier like a “maze” to restrict the escape of molecules during the combustion process. Hence, the reduction of pyrolyzed products is probably due to the physical barrier effect endowed by MXene-based frameworks with maze-like structure.

Here we also carried out the micro-combustion calorimeter test to evaluate the flame retardancy of the as-prepared membranes. As presented in Fig. 6a, PVA and PVB both show a single peak heat release rate (HRR) curve with a peak HRR of about 508.4 W/g and 511.7 W/g at the temperature of 268 ℃ and 416 ℃ respectively. After adding HPUPO, the peak HRR of PVB/HPUPO was reduced to 340.4 W/g about 33.5% off compared to the control PVB. For PVA/MXene aerogel, it shows a low pHRR of about 101.4 W/g, which will play as a flame retardant to improve the fire safety of PVB composites. In terms of PVB/HPUPO/MXene membrane, the peak HRR was significantly decreased to 184.5 W/g about 64.0% and 45.9% reduction compared to pristine PVB and PVB/HPUPO membranes respectively. The results can be concluded that the addition of HPUPO can obviously improve the flame retardancy of PVB and the incorporation of MXene-based frameworks can further immensely reduce the heat release rate.

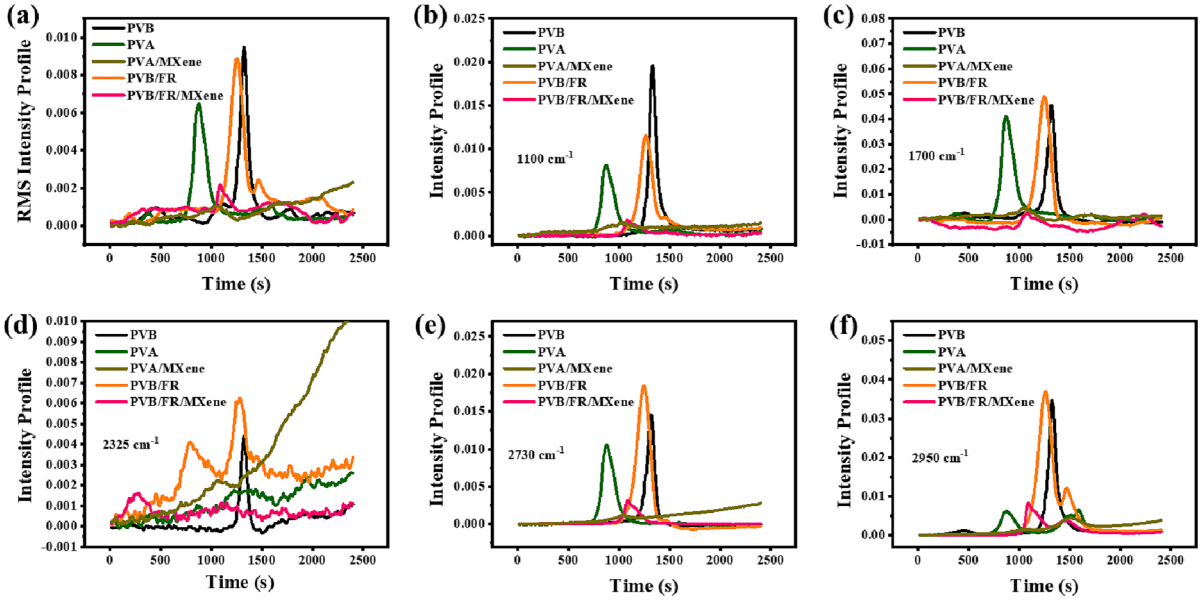

Fig. 5. The analysis of volatiles during thermal degradation for various membranes. a) Absorbance of pyrolyzed volatiles during thermal degradation (Gram-Schmidt) and specific gaseous products including b) ethers; c) carbonyl compounds; d) CO_2; and C–H stretching originated from e) aldehydes and f) alkanes. (For interpretation of the references to colour in this figure legend, the reader is referred to the web version of this article.)

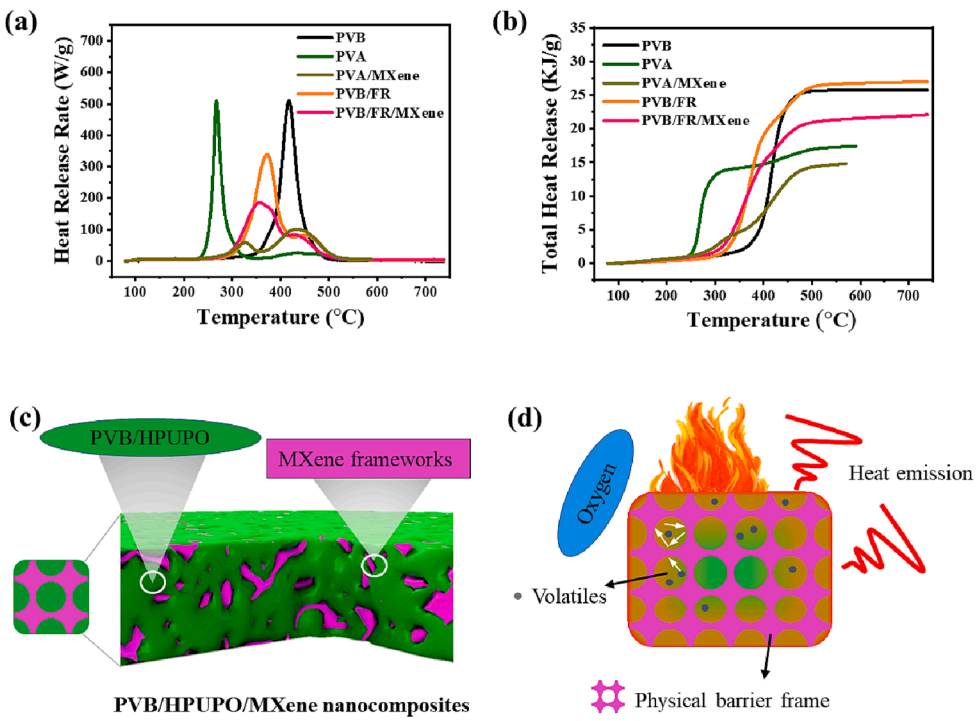

Fig. 6. The flame retardancy of the prepared PVA, PVA/MXene and PVB based membranes. a) Heat release rate of PVA, PVA/MXene and PVB-based membranes; b) Total heat release of PVA, PVA/MXene and PVB-based membranes. The flame retardancy mechanism of PVB/HPUPO/MXene membrane. c) The schematic illustration of PVB/HPUPO/MXene structure with MXene-based frameworks; d) The plausible flame retardancy mechanism. (For interpretation of the references to colour in this figure legend, the reader is referred to the web version of this article.)

As depicted in Fig. 6b, PVB/HPUPO membrane shows a slightly higher total heat release (THR) about 27.0 KJ/g than PVB (25.9 KJ/g). In the case of PVB/HPUPO/MXene, it shows a lower THR value of about 21.8 KJ/g exhibiting an obviously improved flame retardancy. The results analysed above confirm that the flame retardancy mechanism of HPUPO and MXene-based frameworks differ. As for HPUPO, combined with the results from TGA analysis, it can be concluded that HPUPO containing flame retardant phosphorus and nitrogen structures cannot stop the combustion of polymer matrix, but can delay the heat release and improve the fire safety of PVB composites. From the similar residue in the TGA test and THR value compared to pristine PVB, PVB/HPUPO will finally be degraded and release the same amount of heat. What's different is that MXene-based frameworks can significantly retard the release of toxic gaseous and heat and reduce the THR value. This means that MXene-based frameworks can effectively partially stop the degradation process and finally achieve significantly reduced peak HRR and THR values, which is also consistent with the results of TGA.

So based on the above analysis, the flame retardancy mechanism can be summarized below. This work is mainly designed to apply MXene in hydrophobic polymers and combines the advantages of MXene and conventional flame-retardant systems to realise advanced flame-retardant polymer composites. As introduced in Fig. 6c, although MXene can hardly achieve a good dispersion in hydrophobic polymers, it may be fabricated to prepare MXene-based frameworks first and then incorporated with PVB/HPUPO to realise advanced flame retardant PVB composite membrane. Here HPUPO is used to study the synergistic effect of conventional phosphorous and nitrogen-based flame retardants and MXene frameworks on the fire safety of composites and further demonstrate the flame-retardant mechanisms. As depicted in Fig. 6d, it has been verified by TGA, TG-IR and MCC results that HPUPO can retard the heat release during the combustion due to the flame inhibition effect of the released phosphine and phosphine oxide from HPUPO but cannot significantly reduce the total intensity of volatiles and total heat release [18]. Fortunately, introducing MXene-based frameworks can play an important role in improving flame retardancy. MXene frameworks may form an effective physical barrier to suppress the transfer of heat, pyrolyzed products and oxygen, confirmed by the above results. Therefore, it can be regarded that the preparation of MXene-based frameworks can work together with conventional flame retardant to offer a synergistic effect to endow hydrophobic polymers with significantly improved fire safety. The strategy to prepare MXene-based frameworks and phosphorous and nitrogen-based flame retardant systems to enhance the flame retardancy of hydrophobic polymers is feasible and can be used to improve the fire safety of other hydrophobic polymers.

4. Conclusion

In this work, we designed a flexible and thin MXene-based frameworks that was used to realise the fire-safe hydrophobic polymer composite membrane. The framework was created using a simple two-step process involving phase change and freeze-drying. The results demonstrated that the MXene-based framework effectively enhanced the thermal stability of PVB membranes while reducing pyrolyzed volatiles and HPUPO could obviously suppress the heat release rate. Additionally, the PVB/HPUPO/MXene membrane utilizing the MXene-based framework showed a 64.0% and 45.9% reduction in peak heat release rate compared to control PVB and PVB/HPUPO membranes, respectively. On top of HPUPO, the MXene-based framework due to its unique structural advantages also demonstrated the potential to significantly reduce the total heat release and improve the flame retardancy of PVB composite membranes. Therefore, the results revealed that MXene networks and HPUPO could have synergistic effect in improving the thermal stability an reducing the pyrolyzed volatiles, pHRR and THR for PVB composites. Overall, this study addressed the incompatibility between MXene and hydrophobic polymers by introducing a simple and feasible method to prepare MXene-based frameworks that can be well-dispersed in PVB substrates, thereby constructing advanced physical barriers. The results supported the conceptual design and confirmed the high feasibility of this strategy as a new route to create advanced flame-retardant hydrophobic polymer composites using MXene nanosheets.

CRediT authorship contribution statement

Wei Wang: Conceptualization, Methodology, Investigation, Writing – original draft, Writing – review & editing, Funding acquisition. **Cheng Wang:** Writing – review & editing. **Anthony Chun Yin Yuen:**

Resources, Validation. **Ao Li:** Validation. **Bo Lin:** Validation. **Yao Yuan:** Visualization. **Chao Ma:** Supervision, Methodology, Project administration. **Yu Han:** Resources, Supervision, Methodology. **Guan Heng Yeoh:** Resources, Funding acquisition, Supervision.

Declaration of Competing Interest

The authors declare that they have no known competing financial interests or personal relationships that could have appeared to influence the work reported in this paper.

Data availability

Data will be made available on request.

Acknowledgement

This research was supported under Australian Research Council/ Discovery Early Career Researcher Award (DECRA) funding scheme (project number DE230100180); This work was also sponsored by the Australian Research Council (ARC Industrial Transformation Training Centre IC170100032)

Appendix A. Supplementary data

Supplementary data to this article can be found online at https://doi.org/10.1016/j.compositesa.2023.107673.

References

[1] Jin X, Wang J, Dai L, Liu X, Li L, Yang Y, et al. Flame-retardant poly (vinyl alcohol)/MXene multilayered films with outstanding electromagnetic interference shielding and thermal conductive performances. Chem Eng J 2020;380:122475.
[2] Li L, Liu X, Wang J, Yang Y, Cao Y, Wang W. New application of MXene in polymer composites toward remarkable anti-dripping performance for flame retardancy. Compos Part A Appl Sci Manuf 2019;127:105649.
[3] Yang W, Liu J-J, Wang L-L, Wang W, Yuen ACY, Peng S, et al. Multifunctional MXene/natural rubber composite films with exceptional flexibility and durability. Compos Part B 2020;188:107875.
[4] Anasori B, Lukatskaya MR, Gogotsi Y. 2D metal carbides and nitrides (MXenes) for energy storage. Nat Rev Mater 2017;2(2):1–17.
[5] Chen W, Liu L-X, Zhang H-B, Yu Z-Z. Kirigami-inspired highly stretchable, conductive, and hierarchical Ti3C2T x MXene films for efficient electromagnetic interference shielding and pressure sensing. ACS Nano 2021;15(4):7668–81.
[6] Li X, Huang Z, Shuck CE, Liang G, Gogotsi Y, Zhi C. MXene chemistry, electrochemistry and energy storage applications. Nat Rev Chem 2022;6(6):389–404.
[7] Wan S, Li X, Chen Y, Liu N, Du Y, Dou S, et al. High-strength scalable MXene films through bridging-induced densification. Science 2021;374(6563):96–9.
[8] Wang W, Yuen ACY, Long H, Yang W, Li A, Song L, et al. Random nano-structuring of PVA/MXene membranes for outstanding flammability resistance and electromagnetic interference shielding performances. Compos Part B 2021;224:109174.
[9] Zhou Z, Zheng N, Sun W. Self-interlocked MXene/polyvinyl alcohol aerogel network to enhance interlaminar fracture toughness of carbon fibre/epoxy composites. Carbon 2023;201:60–70.
[10] Zhang Z, Cao H, Quan Y, Ma R, Pentzer EB, Green MJ, et al. Thermal stability and flammability studies of MXene–organic hybrid polystyrene nanocomposites. Polymers 2022;14(6):1213.
[11] Liu C, Yao A, Chen K, Shi Y, Feng Y, Zhang P, et al. MXene based core-shell flame retardant towards reducing fire hazards of thermoplastic polyurethane. Compos Part B 2021;226:109363.
[12] Zhang L, Huang Y, Dong H, Xu R, Jiang S. Flame-retardant shape memory polyurethane/MXene paper and the application for early fire alarm sensor. Compos Part B 2021;223:109149.
[13] Tang T, Wang S, Jiang Y, Xu Z, Chen Y, Peng T, et al. Flexible and flame-retarding phosphorylated MXene/polypropylene composites for efficient electromagnetic interference shielding. J Mater Sci Technol 2022;111:66–75.
[14] Sun R, Zhang HB, Liu J, Xie X, Yang R, Li Y, et al. Highly conductive transition metal carbide/carbonitride (MXene)@ polystyrene nanocomposites fabricated by electrostatic assembly for highly efficient electromagnetic interference shielding. Adv Funct Mater 2017;27(45):1702807.
[15] Luo J-Q, Zhao S, Zhang H-B, Deng Z, Li L, Yu Z-Z. Flexible, stretchable and electrically conductive MXene/natural rubber nanocomposite films for efficient electromagnetic interference shielding. Compos Sci Technol 2019;182:107754.
[16] Xu M-K, Liu J, Zhang H-B, Zhang Y, Wu X, Deng Z, et al. Electrically conductive Ti3C2T x MXene/polypropylene nanocomposites with an ultralow percolation threshold for efficient electromagnetic interference shielding. Ind Eng Chem Res 2021;60(11):4342–50.
[17] Ma C, Yu B, Hong N, Pan Y, Hu W, Hu Y. Facile synthesis of a highly efficient, halogen-free, and intumescent flame retardant for epoxy resins: thermal properties, combustion behaviors, and flame-retardant mechanisms. Ind Eng Chem Res 2016;55(41):10868–79.
[18] Ma C, Qiu S, Wang J, Sheng H, Zhang Y, Hu W, et al. Facile synthesis of a novel hyperbranched poly (urethane-phosphine oxide) as an effective modifier for epoxy resin. Polym Degrad Stab 2018;154:157–69.
[19] Ghidiu M, Lukatskaya MR, Zhao M-Q, Gogotsi Y, Barsoum MW. Conductive two-dimensional titanium carbide 'clay'with high volumetric capacitance. Nature 2014;516(7529):78–81.
[20] Xuan J, Wang Z, Chen Y, Liang D, Cheng L, Yang X, et al. Organic-base-driven intercalation and delamination for the production of functionalized titanium carbide nanosheets with superior photothermal therapeutic performance. Angew Chem 2016;128(47):14789–94.